

The relative transmission of THz pulses is also measured with respect to the gate voltage and is shown in Fig. 3. The transmission decreases linearly proportional to the positive voltage. The best fit to this transmission versus voltage plot is obtained with a damping rate of 10 THz. Consequently, it gives a mobility of  $110 \text{ cm}^2/\text{V}\cdot\text{sec}$ .

We have shown that the MOS inversion layer mobility can be measured without source and drain contacts using freely-propagating THz electromagnetic pulses. Potential applications include rapid in-line process control and monitoring of the effect of subsequent high-temperature process steps on mobility. Also, high-field phenomena in inversion layers can be studied utilizing high-power THz pulses.<sup>3</sup>

<sup>3</sup>Department of Physics

1. M. van Exter, D. Grischkowsky, Phys. Rev. B 41, 12140 (1990).
2. W. J. Walecki, D. Some, V. G. Kozlov, A. V. Nurmikko, Appl. Phys. Lett. 63, 1809 (1993).
3. E. Budiarto, S. Jeong, J. Son, J. Margolies, J. Bokor, in Proceedings IEEE LEOS, 1995 Annual Meeting, paper UOE5.2.

CTuD5

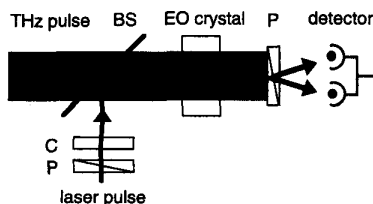
9:15 am

**Ultrafast electro-optic field sensors for terahertz beams**

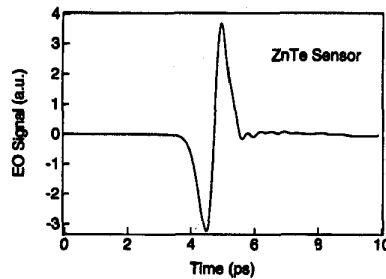
Q. Wu, P. Campbell, X.-C. Zhang, L. Libelo,\* Physics Department, Rensselaer Polytechnic Institute, Troy, New York 12180-3590

To date, the measurement of terahertz pulse is primarily being carried out using ultrafast photoconductive antennas and far-infrared interferometric techniques. In this presentation, we report our recent work on ultrafast electro-optic field sensors for the coherent measurement of freely-propagating THz beams. The sensitivity of our ultra-wideband field sensors is improved to be comparable with the ultrafast photoconductive dipole antennas currently used.

Figure 1 illustrates free-space electro-optic sampling with an electro-optic sensor in the a collinear configuration. An 1" pellicle beamsplitter, which is transparent for the terahertz beam and the pre-focused optical probe beam on the



CTuD5 Fig. 1 Free-space electro-optic sampling with an electro-optic field sensor in the a collinear configuration.



CTuD5 Fig. 2 Time-resolved electro-optic signal measured using a (110) oriented ZnTe crystal.

electro-optic crystal is about 10 mm and 0.2 mm, respectively. This arrangement is similar to what would be used in a terahertz imaging system where the probe beam spot (pixel size) is comparable with the terahertz wavelength. A polarizer (P), and compensator (C) are used to convert the induced phase retardation of the probe beam into an intensity modulation. During the measurement, the power ratio of the optical pump/probe beam is about 10,000.

Figure 2 plots a time-resolved electro-optic signal from a 1.5-mm-thick (110) oriented ZnTe crystal. Typically, the single-scan SNR in a lock-in amplifier with the time-constant set at 0.3 sec is better than 1000-to-1. Due to the dispersion in ZnTe, the waveform of electro-optic signal in Fig. 2 has a time-averaging effect. Improved velocity-matching configurations will allow us to increase the interaction length and thus further improve the both detection sensitivity and temporal resolution.

Theoretically, if we can resolve photomodulation  $\Delta I/I$  as small as  $10^{-7}$  and if  $\Delta I/I = 1$  corresponds to 100% modulation, then the linear dynamic range of this electro-optic detection can be as large as  $10^6$ . This sensitivity is comparable or better than that from the best photoconductive dipole antenna currently available. The superior SNR of the electro-optic sensor-based detection system allows us to measure terahertz radiation with a shorter lock-in time constant. For example, a SNR better than 50 can be achieved directly from an oscilloscope attached to the lock-in amplifier with a time constant of 10 ms.

In conclusion, the sensitivity and bandwidth of an ultrafast electro-optic field sensor can be comparable with a standard photoconductive dipole antenna. Our preliminary results demonstrate the advantages of using the linear electro-optic effect (Pockels effect) for the measurement of ultrafast far-infrared subpicosecond electromagnetic radiation. We also proved the feasibility of using an electro-optic sensor for real-time 2-D subpicosecond far-infrared imaging.

\*AMSRL-WT-NH, Army Research Laboratory, Adelphi, Maryland 20783

CTuD6

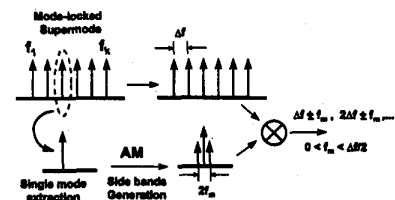
9:30 am

**Novel optoelectronic technique for tunable millimeter-wave generation using a monolithic mode-locked semiconductor laser**

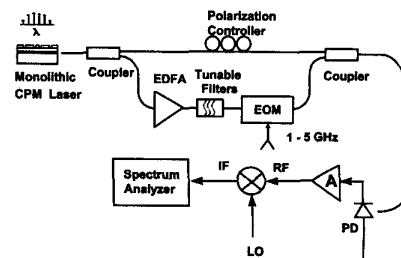
Dennis T. K. Tong, Neel A. Bhatt, Ming C. Wu, UCLA, Electrical Engineering Department, Box 951594, Los Angeles, California 90095-1594

Optoelectronic generation and processing of continuously tunable millimeter-wave are required in many analog optical-fiber transmission systems. Conventionally, microwave signals can be generated by optical heterodyning of two distributed feedback (DFB) laser wavelengths with optical phase-lock loop.<sup>1</sup> Such approach provides wide tuning range but becomes difficult at higher frequencies  $> 20 \text{ GHz}$  due to the broad linewidth of semiconductor lasers. Monolithic mode-locked semiconductor laser with repetition frequencies range from a few GHz to several hundred GHz are ideal for generating millimeter-waves with fixed frequencies.<sup>3</sup> In this paper, we propose and experimentally demonstrate a novel optoelectronic technique for continuously tunable millimeter-wave generation in which a mode-locked laser diode is employed in conjunction with an external electro-optic modulator (EOM) to generate millimeter-wave signal up to over 100 GHz.

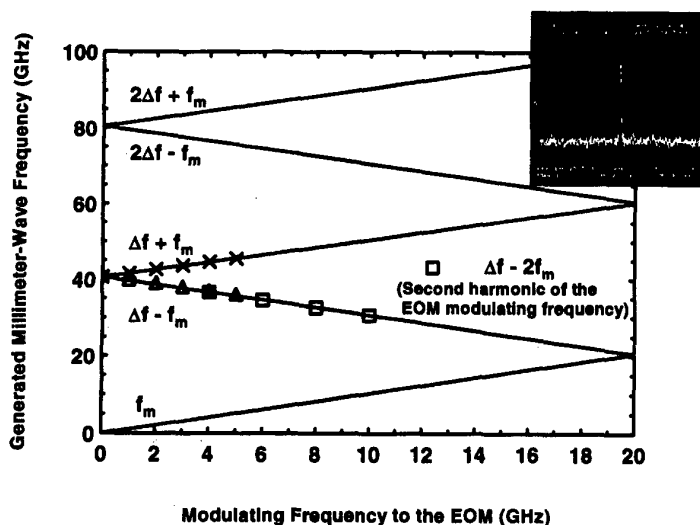
The principle of the proposed scheme is illustrated in Fig. 1. The mode-locked laser diode provides a mode-locked "supermode"  $\{f_1, f_2, \dots, f_k\}$  with mode spacing  $\Delta f$  defined by the mode-locking frequency. It has been shown that the individual mode  $f_i$  can be extracted from the supermode with side-mode-suppression-ratio larger than 40 dB.<sup>2</sup> The ex-



CTuD6 Fig. 1 Operating principle of the proposed optoelectronic scheme for millimeter-wave generation.



CTuD6 Fig. 2 Experimental setup for optoelectronics generation of millimeter-wave using a monolithic CPM laser and external EO modulator.



CTuD6 Fig. 3 Generated millimeter-wave frequencies as a function of the modulating frequency to the EO modulator. The cross, triangle, and square represents experimental results. The inset shows the RF spectrum at 35 GHz.

tracted mode is amplitude-modulated to an RF frequency  $f_m$  by the EOM to generate sideband frequencies  $f_+^{\pm}$  and  $f_-^{\pm}$ , where  $f_{\pm}^{\pm} = f_i \pm f_m$ . The modulated wavelength is then recombined with the original mode-locked spectrum. Because  $f_{\pm}^{\pm}$  and  $f_{1,2,\dots,k}$  are phase-locked together, upon mixing on the photodetector, RF signals with frequencies of  $\Delta f \pm f_m$ ,  $2\Delta f \pm f_m$ , ... etc. are generated. If  $f_m$  can vary from 0 to  $\Delta f/2$ , a continuously tunable optoelectronic millimeter-wave source up to over 100 GHz can be realized.

The experimental setup is shown in Fig. 2. A 40-GHz monolithic colliding-pulse mode-locked (CPM) InGaAs/InGaAsP quantum well laser is used to provide the mode-locked supermode. The mode-locked signal is divided into two branches. The lower branch is amplified by an EDFA (17 m of Corning ER-22) to an average optical power of 8 dBm. The center mode is selected by a fiber Fabry-Perot filter and is launched into the EOM (BW = 5 GHz) for amplitude modulation. The modulated wavelength is then recombined with the mode-locked spectrum by a 3-dB coupler. A photodetector with 34-GHz bandwidth is employed to detect the heterodyned signal. Figure 3 displays the generated millimeter-wave frequency as a function of the modulating frequency to the EOM. Millimeter-wave from 35 to 45 GHz are experimentally generated. To extend the modulating frequency over the bandwidth of the EOM, it is biased at the peak transmission to generate the second harmonic of the modulating frequency. Range of millimeter-wave frequencies are extended to from 30 to 50 GHz. The frequencies and higher are not observed due to photodetector bandwidth. The phase noises of millimeter-wave signals, generated by the fundamental and the second-harmonic modulating frequencies, are  $-54$  dBc/Hz and  $-39$  dBc/Hz, respectively. These figures are limited by

system noise, and can be improved by increasing the optical powers. Further results will be discussed in the conference.

In conclusion, a novel optoelectronic scheme for continuously tunable millimeter-wave generation is proposed and experimentally demonstrated for 30 GHz to 50 GHz. This technique has a potential tuning range of over 100 GHz. This work is supported in part by ARPA NCIPT and Packard Foundation.

1. U. Gliese, E. Lintz Christensen, K. E. Stubkjaer, J. Lightwave Technol. 9, 779-790 (1991).
2. D. T. K. Tong, M. C. Wu, IEEE/LEOS 1995 Summer Topical Meeting, August 7-11, 1995, Keystone, Colo., paper ThC4.
3. K. Y. Lau, IEEE J. Quantum Electron. 26, 250-261 (1990).

CTuD7 9:45 am

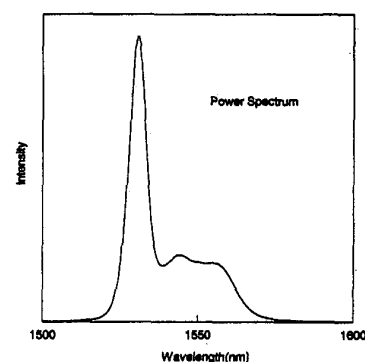
#### Pulse shaping of incoherent light by use of a liquid crystal modulator array

V. Binrajka, C.-C. Chang, A. W. R. Emanuel, D. E. Leaird, A. M. Weiner, School of Electrical and Computer Engineering, Purdue University, 1285 EE Building, West Lafayette, Indiana 47907

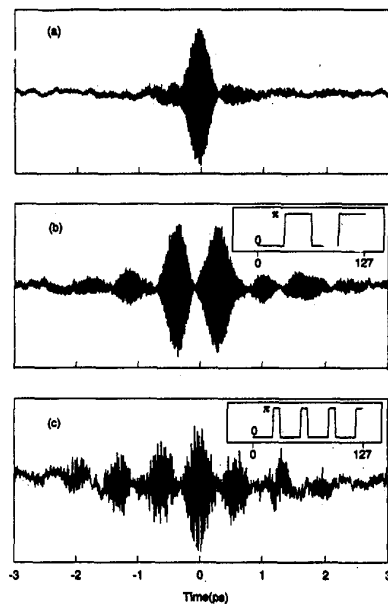
We apply femtosecond pulse shaping techniques<sup>1,2</sup> for electronically programmable phase filtering of broadband incoherent light at 1.5  $\mu\text{m}$ . Pulse shaping applied to incoherent light results in tailoring of the electric field coherence function, in contrast to the pulse intensity and phase profile, as in the usual coherent femtosecond pulse-shaping experiments. Our results may be important for broadband communications using coherence coding for time-division multiplexed data transmission<sup>3</sup> or code-division networking.<sup>4,5</sup>

In our experiment we used an erbium-fiber laser operating below thresh-

old as the source for broad-band incoherent light in the 1.5- $\mu\text{m}$  optical-fiber communications bands. A typical spectrum from the source is shown in Fig. 1. The light from the source was sent to a Michelson interferometer for field correlation measurements. A standard femto-second pulse shaper<sup>1,2</sup> was introduced in one arm of the Michelson interferometer. A liquid crystal modulator (LCM) array with 128 pixels was used as an electronically programmable pulse-shaping mask. The phase pattern applied by the LCM array alters the coherence function of the incoming incoherent light. We measure this coherence function by recording the interference fringes in the output power from the Michelson interferometer as the



CTuD7 Fig. 1 Power spectrum from the incoherent broad-band Er-fiber ASE source.



CTuD7 Fig. 2 (a) Electric field autocorrelation of the input incoherent broad-band light. (b), (c) The field cross-correlations between the source and the light modified by the pulse-shaper. The applied phase masks are shown in the insets. Phase jumps are  $\pi$ .